OPEN

A combination of high dose rate (10X FFF/2400 MU/min/ 10 MV X-rays) and total low dose (0.5 Gy) induces a higher rate of apoptosis in melanoma cells *in vitro* and superior preservation of normal melanocytes

Sreeja Sarojini[a], Andrew Pecora[b], Natasha Milinovikj[a], Joseph Barbiere[b], Saakshi Gupta[a], Zeenathual M. Hussain[a], Mehmet Tuna[b], Jennifer Jiang[a], Laura Adrianzen[a], Jaewook Jun[a], Laurice Catello[b], Diana Sanchez[a], Neha Agarwal, Stephanie Jeong[a], Youngjin Jin[a], Yvonne Remache[a], Andre Goy[b], Alois Ndlovu[b], Anthony Ingenito[b] and K. Stephen Suh[a]

The aim of this study was to determine the apoptotic effects, toxicity, and radiosensitization of total low dose irradiation delivered at a high dose rate *in vitro* to melanoma cells, normal human epidermal melanocytes (HEM), or normal human dermal fibroblasts (HDF) and to study the effect of mitochondrial inhibition in combination with radiation to enhance apoptosis in melanoma cells. Cells irradiated using 10X flattening filter-free (FFF) 10 MV X-rays at a dose rate of 400 or 2400 MU/min and a total dose of 0.25–8 Gy were analyzed by cell/colony counting, MitoTracker, MTT, and DNA-damage assays, as well as by quantitative real-time reverse transcriptase PCR in the presence or absence of mitochondrial respiration inhibitors. A dose rate of 2400 MU/min killed on average five-fold more melanoma cells than a dose rate 400 MU/min at a total dose of 0.5 Gy and preserved 80% survival of HEM and 90% survival of HDF. Increased apoptosis at the 2400 MU/min dose rate is mediated by greater DNA damage, reduced cell proliferation, upregulation of apoptotic genes, and downregulation of cell cycle genes. HEM and HDF were relatively unharmed at 2400 MU/min. Radiation induced upregulation of mitochondrial respiration in both normal and cancer cells, and blocking the respiration with inhibitors enhanced apoptosis only in melanoma cells. A high dose rate with a low total dose (2400 MU/min, 0.5 Gy/10X FFF 10 MV X-rays) enhances radiosensitivity of melanoma cells while reducing radiotoxicity toward HEM and HDF. Selective cytotoxicity of melanoma cells is increased by blocking mitochondrial respiration. *Melanoma Res* 25:376–389

Melanoma Research 2015, **25**:376–389

Keywords: 2400 MU/min, apoptosis, cancer, dose rate, flattening filter-free mode, melanoma, melanoma radiotherapy, mitochondrial respiration, primary melanocytes

[a]The Genomics and Biomarkers Program, University Medical Center and [b]Clinical Division, Hackensack University Medical Center, The John Theurer Cancer Center, Hackensack, New Jersey, USA

Correspondence to K. Stephen Suh, PhD, The Genomics and Biomarkers Program, David Jurist Research Building, The John Theurer Cancer Center, 40 Prospect Avenue, Hackensack, NJ 07601, USA
Tel: +1 551 996 8214; fax: +1 551 996 8776;
e-mail: ksuh@hackensackumc.org

Received 8 September 2014 **Accepted** 5 May 2015

Introduction

Risk factors for melanoma include dysplastic nevi syndrome, continuous solar ultraviolet radiation exposure, family history of melanoma, sunburns, *BRAF* gene mutation, and White ancestry [1]. Malignant melanoma is highly aggressive, chemoresistant, and poorly radioresponsive, and is responsible for as much as 80% of the mortality among all skin cancers; it has a 5-year survival rate of 14% [2]. Melanoma can arise from skin, eyes, mucosa, or the central nervous system [3]. Patients diagnosed with thin lesions (<1 mm) have an increased cure rate after surgery, but 5% develop metastatic melanoma, which limits 10-year survival [4]. Therapy for metastatic melanoma has improved with the understanding of melanoma signaling pathways and the identification of tumor cell targets in the cell. Identification of small molecules that interfere with key signaling pathways has helped the progress of new therapeutic approaches in melanoma [5].

Among these, radiotherapy treatments reduce the rate of recurrence, improve control of local disease, and limit metastasis to the bone or brain [6]. Melanoma metastasizes to the brain in 10–40% of cases [7]. Recent management protocols for melanoma incorporate chemotherapy, immunotherapy, and radiotherapy [1,8].

Mutation of the *BRAF* gene is a common risk factor for melanoma [9]. *BRAF* acts as a mitogen-activated protein

DOI: 10.1097/CMR.0000000000000174

kinase kinase kinase [10] in the ERK pathway network [11] and regulates cell growth, differentiation, and survival [12]. *BRAF V600E* is the most common mutation; it occurs in more than 50% of all melanoma cases and leads to hyperactive kinase [13–15]. Family atypical multiple mole melanoma syndrome is caused by a familial autosomal dominant gene [16] and is associated with a large number of atypical nevi typically presenting as cutaneous melanoma [17].

Radiotherapy can be an effective treatment for melanoma, but radioresistance of melanoma cells affects clinical outcomes [18]. In the past few years, modern linear accelerators operating in a flattening filter-free (FFF) mode and having increased dose rate capabilities have improved radiotherapy, with advantages over conventional radiotherapy including shortened dose delivery time, lower dose delivery outside the field, shorter treatment period, and lower rates of secondary malignancies [19]. In addition, improved image guidance, along with volumetric-modulated arc therapy capabilities, has improved target conformity, while reducing exposure of normal tissue surrounding the lesion. The ability to deliver radiation in a concave isodose profile to minimize injury to normal surrounding tissue represents a significant advance in radiotherapy [20]. Maintaining a high survival rate among normal cells subsequent to radiation treatment is a crucial component of all radiotherapies, and various in-vitro conditions have been tested [21].

Aberrations in mitochondrial functions resulting in deregulation of cellular aerobic respiration, differentiation, and proliferation have been reported in multiple malignancies including breast, colon, lung, liver, and kidney cancers, and leukemia and lymphoma [22], as well as in many neurological disorders [23]. Inhibition of mitochondrial respiration or oxidative phosphorylation increases therapeutic efficiency in some *in-vitro* and *in-vivo* models [24], and it has been suggested that an increase in the tumoricidal efficacy of radiotherapy can be achieved by targeting the mitochondria [25].

In a direct *in-vitro* comparison between a conventional dose rate (400 MU/min) and an unconventional dose rate (2400 MU/min) coupled with a low total dose (0.5 Gy) of 10X FFF 10 MV X-rays, we found a significant improvement in the survival of normal cells and a concurrent increase in apoptosis in melanoma cells. Titrated doses of inhibitors to the mitochondrial respiratory chain increased the radiosensitivity of melanoma cells while maintaining normal melanocyte survival. Treatment of melanoma cells *in vitro* with the unconventional dose rate (FFF mode at 2400 MU/min) and low dose radiation protocol (0.5 Gy) has not been reported yet. Our radiation delivery protocol in the engineered mode of the intensity-modulated radiotherapy device and associated hardware/software can potentially translate to the clinical setting. Our results support the investigation of novel radiotherapeutic options and open doors to the untested field of radiotherapy research.

Methods

Cell culture

Melanoma cell lines (WC00046, WC00060, and WC00081; Fig. 1a) were purchased from Coriell Institute (Camden, New Jersey, USA). Cells were cultured in RPMI containing 10% fetal bovine serum and 1% penicillin/streptomycin (Invitrogen, Grand Island, New York, USA). All melanoma cell lines were positive for BRAF mutation and negative for NRAS mutation, and the WC00046 and WC00081 cell lines were positive for p53 (Fig. 6a). Primary human epidermal melanocytes (HEM) and culture media were purchased from ScienCell (Carlsbad, California, USA), and normal human dermal fibroblasts (HDF) were prepared as previously described [26–28]. Oligomycin and rotenone (50 nmol/l; Sigma Aldrich, St. Louis, Missouri, USA) were used to block mitochondrial respiration.

Radiation

Cells were seeded (5×10^5) in T-25 culture flasks (BD-Falcon; BD-Biosciences, Durham, North Carolina, USA), allowed to adhere overnight, and irradiated with 10 MV X-rays at dose rates of 400 or 2400 MU/min using TrueBeam (Varian Medical Systems, Palo Alto, California, USA) with 10X FFF. The total dose range of 10 MV X-rays was 0.25–8 Gy (100–1000 Gy data not shown) for multiple experiments.

Colony formation assays

One day after irradiation, HEM and melanoma cells were treated with trypsin, resuspended, counted using a Beckman Coulter Counter (Beckman Coulter, Brea, California, USA), and serially diluted (1 : 100, 1 : 1000, and 1 : 10 000) in complete medium for seeding in culture dishes (BD Falcon, Corning, New York, USA). Colonized cells were stained with hematoxylin for 30 min, fixed with 100% ethanol for 30 min, washed in water for clearing the background, dried overnight, and counted [29,30].

RNA isolation and qRT-PCR

RNA was extracted using TRIzol (Invitrogen), and selected genes (Figs 1d and e, 2d and e and 4b were amplified by quantitative real-time reverse transcriptase PCR (qRT-PCR) with SYBR green (Qiagen, Germantown, Maryland, USA) on a FAST Model 7900HT (Applied Biosystems, Foster City, California, USA) as previously published [31]. Primer sequences are given in Table 1. Data were analyzed on SDS 7900HT software v2.2.2 (Applied Biosystems, Grand Island, New York, USA) using the comparative threshold cycle (C_t) method ($2^{-\Delta\Delta C_t}$) for calculating fold changes and SDs [32].

Assays

Migration

A collagen-based cell migration assay (QCM TM 24-well kit; Millipore, Billerica, Massachusetts, USA) was used as described by the manufacturer. Cells (5×10^5 cells/well)

Fig. 1

(a)

Melanoma cell lines			
Identifier	WC000046	WC00060	WC00081
Sample description	Melanoma Malignant	Melanoma Malignant	Melanoma Malignant
Thickness	2.75	0.69	N/A
Pathology	Superficial spreading melanoma (SSM) RGP/VGP	Superficial spreading melanoma (SSM) RGP/VGP	Malignant melanoma, vertical growth phase
Stage	Metastatic stage 2	1	N/A
Mutation	N/A	VAL599ILE	LYS144TER

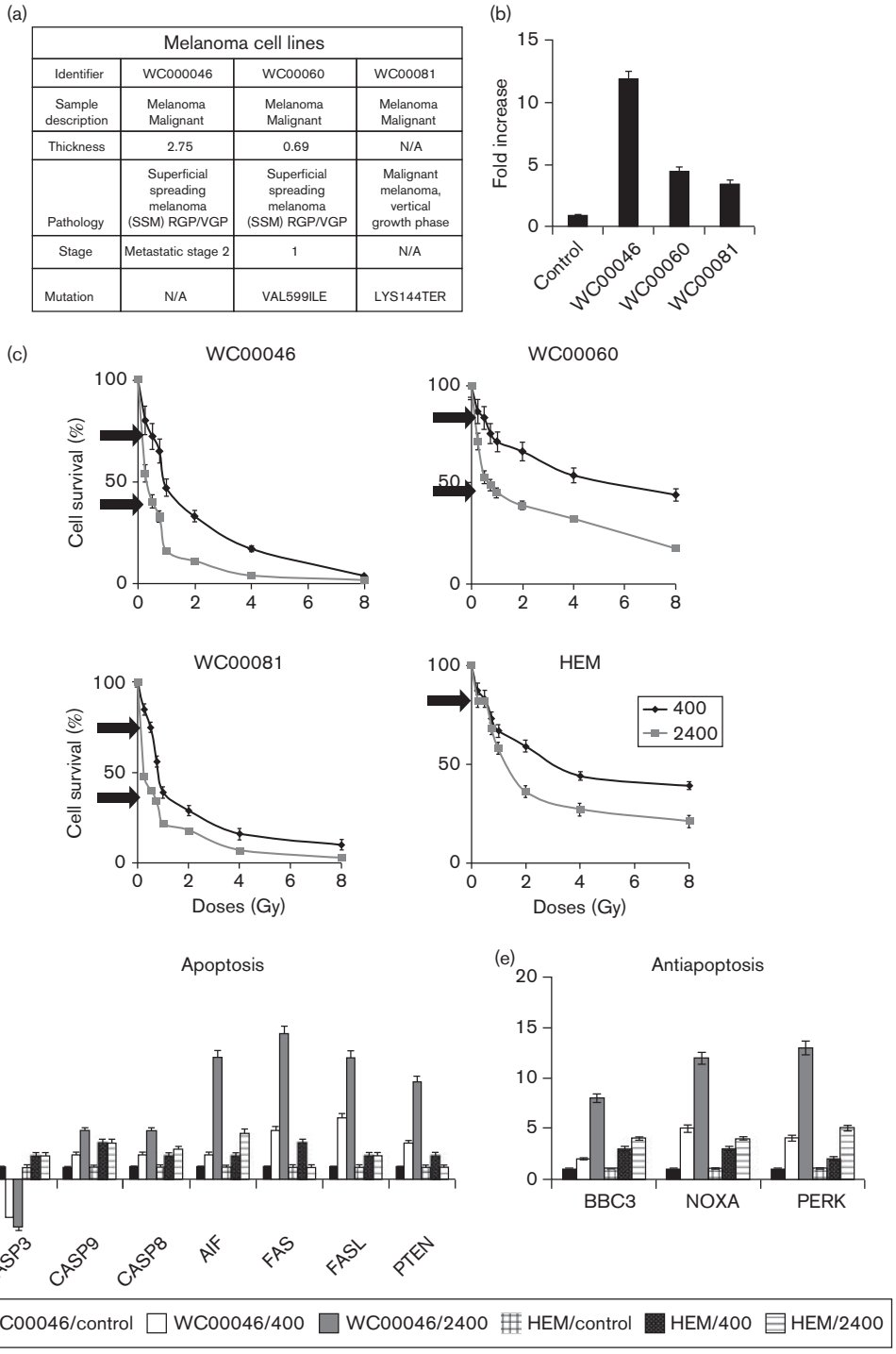

(a) Description of cell lines, including pathology, mutation, and staging. (b) Migration potential of cell lines WC00046, WC00060, and WC00081. Migration assay was conducted using the QCM TM 24-well migration assay kit in melanoma cell lines and normalized against melanocytes (HEM) to validate aggressiveness and metastatic potential. The standard error bars were generated from duplicates of two separate assays. (c) Cells were irradiated with dose rates of 400 or 2400 Mu/min and total doses of 0.25, 0.5, 0.75, 1, 2, 4, or 8 Gy. Cell numbers were determined 7 days after radiation. Black arrows denote the 0.5 Gy dose at both dose rates. The experiment was conducted individually four times. One representative experiment is shown and standard error bars are shown for triplicate assays. Significance of differences between 400 and 2400 MU/min were determined using Student's *t*-test; $P < 0.0005$ for WC00046, $P < 0.002$ for WC00060, $P < 0.001$ for WC00081, and $P < 0.005$ for HEM. Expression of (d) apoptosis genes and (e) ER-stress genes was measured by qRT-PCR in duplicate for cells irradiated under the condition described in (c). Fold changes were calculated by normalization against nonradiated cells corresponding to each cell type. Data representing WC00046/control (solid black), WC00060/400 (solid white), WC00081/2400 (solid grey), HEM/control (large grid), HEM/400 (black dotted), and HEM/2400 (light horizontal) are represented by bars in fold change. ER, endoplasmic reticular; HEM, human epidermal melanocytes; qRT-PCR, quantitative real-time reverse transcriptase PCR.

Fig. 2

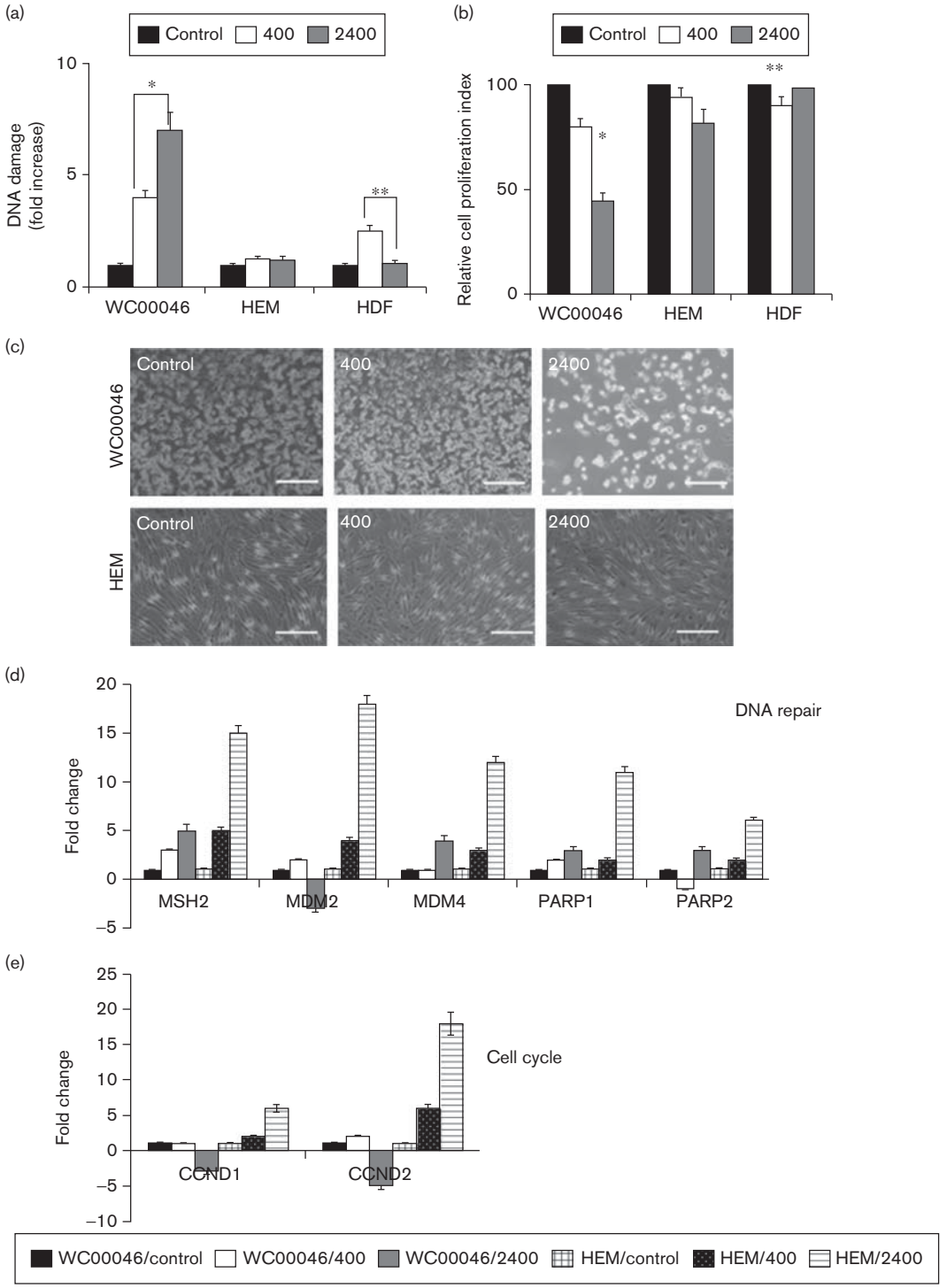

(a) DNA damage of irradiated cells 7 days after irradiation at a total dose of 0.5 Gy for dose rates of 2400 MU/min (solid grey) and 400 MU/min (solid white) normalized against nonirradiated cells (solid black) for each corresponding cell type. Data represent the average of four independent experiments; error bars are shown, and the statistical difference between the two dose rates for WC00046 (*) is $P < 0.002$. (b) Cell proliferation of irradiated cells from (a) quantified using the MTT assay; standard error bars are shown, and the statistical difference between 400 and 2400 MU/min for WC00046 was $P < 0.003$. (c) Images of WC00046 and HEM cells under condition (a) were taken by phase contrast microscopy. The WC00060 and WC00081 cells lines showed similar morphologies (data not shown). Expression of (d) DNA repair genes and (e) cell cycle genes by irradiated cells from (a) was quantified by qRT-PCR. Average fold changes from the four experiments are shown with error bars after normalizing against corresponding nonirradiated control cells. Data representing WC00046/control (solid black), WC00060/400 (solid white), WC00081/2400 (solid grey), HEM/control (large grid), HEM/400 (black dotted), and HEM/2400 (light horizontal) are represented by bars in fold change. HDF, human dermal fibroblasts; HEM, human epidermal melanocytes; qRT-PCR, quantitative real-time reverse transcriptase PCR.

Table 1 Primer sequences for each gene were generated using cDNA sequences from a database (*http://www.ncbi.nlm.nih.gov/gene*) and a web-based software (*http://biotools.umassmed.edu/bioapps/primer3_www.cgi*) for PCR primer designing

Primer sequences used in this study			
NOXA f	gctcaggaacctgactgcat	*Casp 3 f*	gaactggactgtggcattga
NOXA r	ccatcttccgtttccaagg	*Casp 3 r*	tcaagcttgtcggcatactg
Mcl-1 f	ttgctggagtaggagctggt	*Casp 8 f*	gggacaggaatggaacacac
Mcl-1 r	gctaggttgctagggtgcaa	*Casp 8 r*	gccatagatgatgcccttgt
Bcl-2 f	ttccagagacatcagcatgg	*Casp 9 f*	agccacctgagtagcttgga
Bcl-2 r	tgtccctaccaaccagaagg	*Casp 9 r*	agggccctaagaaccagaaa
Bbc-3 f	gacgacctcaacgcacagta	*AIF f*	cctggccaacagcaatactt
Bbc-3 r	gcacctaattgggctccatc	*AIF r*	ctcaagctgggaaccatcat
PERK f	gacctcaagccatccaacat	*FAS f*	cgcaagagtgacacacaggt
PERK r	ttggtccctacttgtcctgtg	*FAS r*	gaaagagcttccccaactcc
ATF 6 f	cacctaaacaaaggggtca	*FASL f*	gagccagacaaatggaggaa
ATF 6 r	tcccaaagtgctgggattac	*FASL r*	aagacagtccccctgaggt
Braf f	cttccgaccagcagatgaag	*MDM4 f*	tctgcccctcttcagacagt
Braf r	ggttgatcctccatcaccac	*MDM4 r*	gaccacttatgcccaggaaa
NDUFS4 f	attggcacaggaccagactc	*PARP 1 f*	gctcctgaacaatgcagaca
NDUFS4 r	tcccatcgctctctggtatc	*PARP 1 r*	tcctgatgatctcggcttct
SDHC v2 f	ttagcaggcatgctgttttg	*SOD2 f*	gggagatgttacagcccagata
SDHC v2 r	ttgggaccctgaatgaagac	*SOD2 r*	agtcacgtttgatggcttcc
UCRC f	attcgctgttggcaagaaac	*TP53 f*	gcgcacagaggaagagaatc
UCRC r	tttgcagagggctttgaagt	*TP53 r*	caaggcctcattcagctctc
COX412 f	gagcttggtgctgaggaaag	*BAX f*	aagctgagcgagtgtctcaa
COX412 r	ccagcttcccttctccttct	*BAX r*	cagttgaagttgccgtcaga
ATPAF2 f	catcacacagggtgaaggtg	*COX f*	cgtggcttgaatgacttcag
ATPAF2 r	ttgggttgtccaatgatgtg	*COX r*	ctcaatgtgaccctcagcaa
PTEN f	gaatggagggaatgctcaga	*GAPDH f*	tcaccagggctgcttttaac
PTEN r	cgcaaacaacaagcagtgac	*GAPDH r*	atgacaagcttcccgttctc
MSH-2 f	ggtgttttgtgccatgtgag	*B2M f*	tgtctttcagcaaggactgg
MSH-2 r	ttggttgcagacctgaggat	*B2M r*	cctccatgatgctgcttaca
CCND1 f	ctctcattcgggatgattgg	*MDM2 f*	cagacggggactagcttttg
CCND1 r	gtgagctggcttcattgaga	*MDM2 r*	ctacttgggaggctgaagca
PARP2 f	ctttgcctctcgcctaaaga	*PARP2 r*	gctggtcctaatggcactgt

All sets of primers were validated for generating one single band of expected size (150 bp) on agarose gel and the template cDNAs were from normal HEM and melanoma cells. Only validated primer sets were used for qRT-PCR analyses. These primer sets were used to generate Figs 1d and e, 2d and e, and 4b.

were seeded and allowed to migrate for 24 h. Cells from the bottom of the insert chamber were collected by trypsin treatment and counted on a Beckman Coulter counter.

Cell proliferation

An MTS assay (Promega, Madison, Wisconsin, USA) was used to measure proliferation of irradiated cells (BioTek Synergy HT, Winooski, Vermont, USA) as described by the manufacturer.

Mitochondrial respiration

Cells were treated with mitotracker Red CMXRos (Invitrogen) and mitochondrial activity was analyzed under a Zeiss Fluorescent microscope (Zeiss, Thornwood, New York, USA) before and after irradiation. Fluorescence was quantified by using ImageJ software.

DNA-damage assay

An EpiQuik in-situ kit (Epigentek, Farmingdale, New York, USA) was used and the cells were grown after irradiation and fixed and permeabilized according to the manufacturer's protocol and previously published literature [33].

Western blotting

Western blotting experiments were carried out [34] using lysates prepared from cell lines (Pierce IP lysis buffer cat# 87788; Invitrogen). SDS-PAGE gels (12%, Criterion TGX Precast Gels) were used to fractionate cell lysates.

Whole-cell extracts were fractionated by SDS-PAGE and transferred onto a polyvinylidene difluoride membrane using a Bio-Rad transfer apparatus (Hercules, California, USA). The membrane was blocked using 5% nonfat dry milk in TBST (10 mmol/l Tris, pH 8.0, 150 mmol/l NaCl, 0.5% Tween 20) for 60 min, it was then washed and incubated with primary antibodies against Bcl-2 (1 : 1000, #7973; Abcam, Cambridge, Massachusetts, USA), *caspase-3* (1 : 2000, H-277), *PARP 1* (1 : 2000, #SC-7148, SC- 8007; Santa Cruz Biotechnology Inc., Santa Cruz, California, USA) and *Actin* (1 : 10 000, AB-6276) at 4°C overnight. The membranes were then washed and incubated with a 1 : 5000 dilution of horseradish peroxidase-conjugated donkey anti-mouse IgGs. The blots were washed and developed using the ECL system.

Flow cytometry

Analysis of the expression of *cyclin D1* and *cyclin D2* (sc-20044 PE, sc-53637 PE; Santa Cruz Biotechnology Inc.) in melanoma cell lines was carried out using Flow cytometry (Gallios; Beckman Coulter) [35,36]. The Per Fix-nc kit (Cat #B3116; Beckman Coulter) was used for fixing, permeabilizing, and preparing the cells for the assay.

Statistical analysis

All experiments were performed a minimum of three times, and the data represent the results of assays performed in triplicate or quadruplicate. Error bars represent 95% confidence intervals. All statistics were based on continuous variables and were obtained using STAT View software (Stat View, Cary, North Carolina, USA). *P*-values less than 0.05 were considered statistically significant. Student's *t*-test was used for comparisons between two groups.

Results

At a total dose of 0.5 Gy, a dose rate of 2400 MU/min killed on average five-fold more melanoma cells than a dose rate of 400 MU/min and preserved 80% survival of normal melanocytes. Three melanoma cell lines (WC00046, WC00060, and WC00081) were chosen on the basis of tumor stage, pathology, and metastatic status (Fig. 1a). The in-vitro migration potential of each cell line was verified as corresponding to the original reported tumor (Fig. 1b). On the basis of cell counts from 7 days after radiation exposure, in-vitro radiation with low total doses (0.25, 0.50, 0.75, and 1 Gy) at a dose rate 2400 MU/min induced significantly higher apoptosis in melanoma cell lines than did a dose rate of 400 MU/min ($P < 0.005$; Fig. 1c). As the total dose increased from 2 to 8 Gy, the difference in cell counts between the two dose rates was reduced significantly for WC00046 and

WC00081 cell lines but not for WC00060 cell line. At 7 days after radiation exposure, the maximum apoptotic differential between 400 and 2400 MU/min occurred at a total dose of 0.5 Gy (Fig. 1c, arrows). Under these conditions, cell killing was 2.1-fold greater for WC00046, three-fold greater for WC00060, and 2.4 fold greater for WC00081 (Fig. 1c). Up to 90% of normal melanocytes survived both radiation dose rates (Fig. 1c). qRT-PCR analysis of apoptotic genes (*Casp 3*, *Casp 9*, *Casp8*, *AIF*, *FAS*, *FASL* and *PTEN*) indicated that Fas-mediated extrinsic cell death signaling was most active in irradiated cells. A dose rate of 2400 MU/min induced an average of 10-fold more apoptosis compared with the control and three-fold more apoptosis compared with the 400 MU/min dose rate (Fig. 1d). Endoplasmic reticular (ER)-stress genes (*BBC-3*, *NOXA*, *PERK*) were upregulated in all cells tested (Fig. 1e). The expression of a radioprotection gene (SOD2) [37] was significantly upregulated in the 2400 MU/min group compared with nonirradiated controls among both melanoma and normal cells. Similar to HEM, normal human fibroblasts maintained higher survival when treated at 2400 MU/min. Cells showed complete recovery from the radiation treatment and continued to proliferate 7 days after irradiation, suggesting that a total dose of 0.5 Gy administered at 2400 MU/min was relatively harmless to HEM and HDF.

A dose rate of 2400 MU/min induced greater DNA damage and reduced cell proliferation compared with a dose rate of 400 MU/min at a total dose 0.5 Gy, but HEM and HDF were relatively unharmed. Quantification of DNA damage in WC00046 cells showed that, at a total dose of 0.5 Gy, the dose rate 2400 MU/min caused seven-fold more DNA damage than in nonirradiated controls and nearly two-fold more DNA damage than a 400 MU/min dose rate ($P < 0.002$; Fig. 2a). WC00060 and WC00081 cell lines showed similar sensitivities (data not shown), suggesting a direct correlation between the dose rate and DNA damage. HEM showed no significant DNA damage and HDF showed slightly higher DNA damage only at the 400 MU/min dose rate (Fig. 2a). When cell proliferation was analyzed at 7 days after radiation, melanoma cells (only WC00046 data shown) irradiated at a rate of 2400 MU/min showed a 2.2-fold reduction in proliferation compared with nonirradiated controls and a 1.7-fold reduction compared with cells irradiated at the 400 MU/min dose rate (Fig. 2b). DNA repair genes (*MSH-2*, *MDM2*, *MDM4*, *PARP 1*, *PARP2*) were upregulated approximately three-fold in the WC00046 cell line treated at 2400 MU/min, which was correlated with DNA damage; however, these genes were upregulated more than 10-fold in HEM compared with controls (Fig. 2c), indicating very active DNA damage control in normal melanocytes. The cell cycle genes CCND1 and CCND2 were downregulated in melanoma cells (only WC00046 data shown; WC00060 and WC00081 showed similar results), but both genes were upregulated six-fold in HEM compared with controls (Fig. 2e). Neither radiation dose rate significantly affected proliferation of HEM (Fig. 2d) or HDF, and the cells continued to maintain normal physiological morphologies. These cells exhibited complete recovery from the radiation treatment and continued to proliferate 7 days after irradiation, suggesting that a total dose of 0.5 Gy administered at 2400 MU/min was relatively harmless to HEM and HDF.

Radiation induced upregulation of mitochondrial respiration by a post-transcriptional mechanism in both normal and cancer cells. Previous reports have indicated that mitochondrial respiration activities were altered after irradiation [38]. To investigate respiration, irradiated melanoma cells were stained with the Mitotracker dye 7 days after irradiation, and fluorescence was qualitatively analyzed (Fig. 3a). Irradiated WC00046 cells showed markedly more fluorescence than nonirradiated controls, and the intensity of staining among cells irradiated at 2400 MU/min was visibly higher than that among cells irradiated at 400 MU/min, suggesting that the radiation directly triggered upregulation of mitochondrial respiration. WC00060 and WC00081 cells gave results similar to WC00046 cells (data not shown). Semiquantitative analysis of the relative fluorescent intensity showed a 1.3-fold increase in cells treated at 400 MU/min and a 2.3-fold increase in cells treated at 2400 MU/min compared with controls, indicating that the increase in fluorescence was directly associated with the radiation dose rate (Fig. 3b). Normal HEM did not show significant upregulation of respiration at either dose rate but HDF showed upregulation. In this setting, images of WC00046 cells that were irradiated and treated with inhibitors showed no significant change in morphology compared with controls (Fig. 3c).

Radiation and mitochondrial respiration inhibitors synergize to induce greater apoptosis in melanoma cells. To investigate whether targeting mitochondrial respiration increased apoptosis in a synergistic manner with radiation, a minimum lethal dose of oligomycin or rotenone was used to pretreat the cells before irradiation. Cell counts 7 days after irradiation showed that apoptosis increased in the presence of the inhibitors for all melanoma cells at both dose rates (Fig. 4a). On average, 76% cell death was observed among cells treated at 2400 MU/min compared with 59% among cells treated at a 400 MU/min dose rate, and cell death among cells treated at 2400 MU/min was 3.6-fold that among nonirradiated controls. In melanocytes, however, the dose of inhibitor used caused apoptosis in less than 20% of cells. In this setting, the expression of major mitochondrial respiratory genes (*NDUFS4*, *SDHC*, *UQCR10*, *ATF6*, *COX412*, and *ATPAF2*) was generally upregulated (Fig. 4b), suggesting that elevated respiratory activity subsequent to radiation treatment was partly a post-transcriptional event. When cell proliferation was

Fig. 3

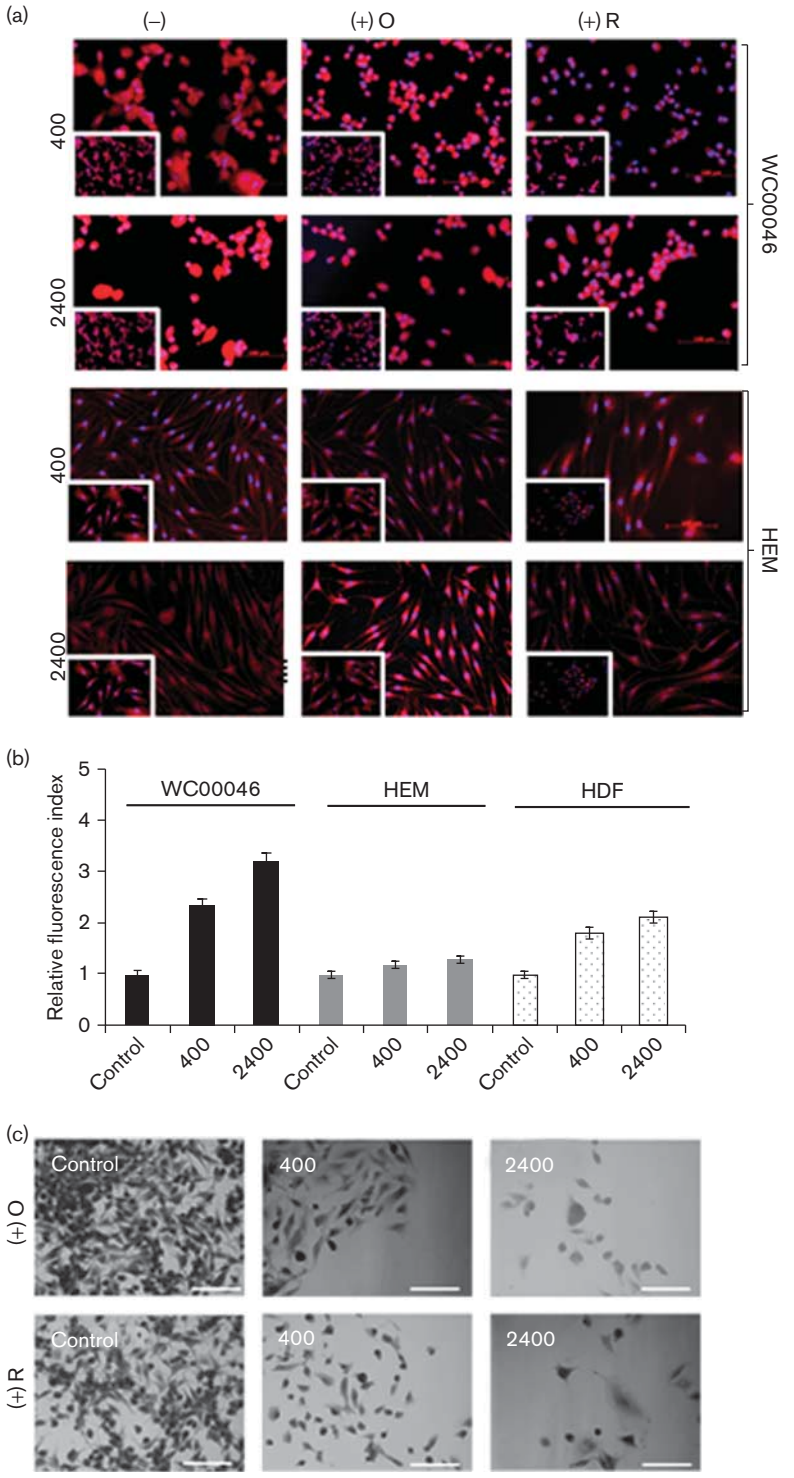

(a) WC00046 melanoma cells and normal HEM were pretreated with oligomycin or rotenone for 1 h and subsequently irradiated with 0.5 Gy at a dose rate of 400 or 2400 MU/min. At 7 days after radiation, the treated cells were stained with Mitotracker red fluorescent dyes to detect mitochondrial respiration, and florescence microscopy was used for imaging (20× magnification; scale bars indicate 100 μm). Nonirradiated control cells (insets) are shown for the individual radiation setting for each cell type. Each panel shows a representative fluorescent field from four separate experiments. (b) Average fluorescence intensity from five random fields for each experimental setting as described in (a) normalized against the average intensity of corresponding nonirradiated cells (black bars). Fold changes for 400 MU/min rate (white bars) and 2400 MU/min rate (grey bars), shown with standard error bars. (c) Cells as in (a) were stained with nuclear red and methylene blue, and morphology was visualized by bright field microscopy. HEM, human epidermal melanocytes.

Fig. 4

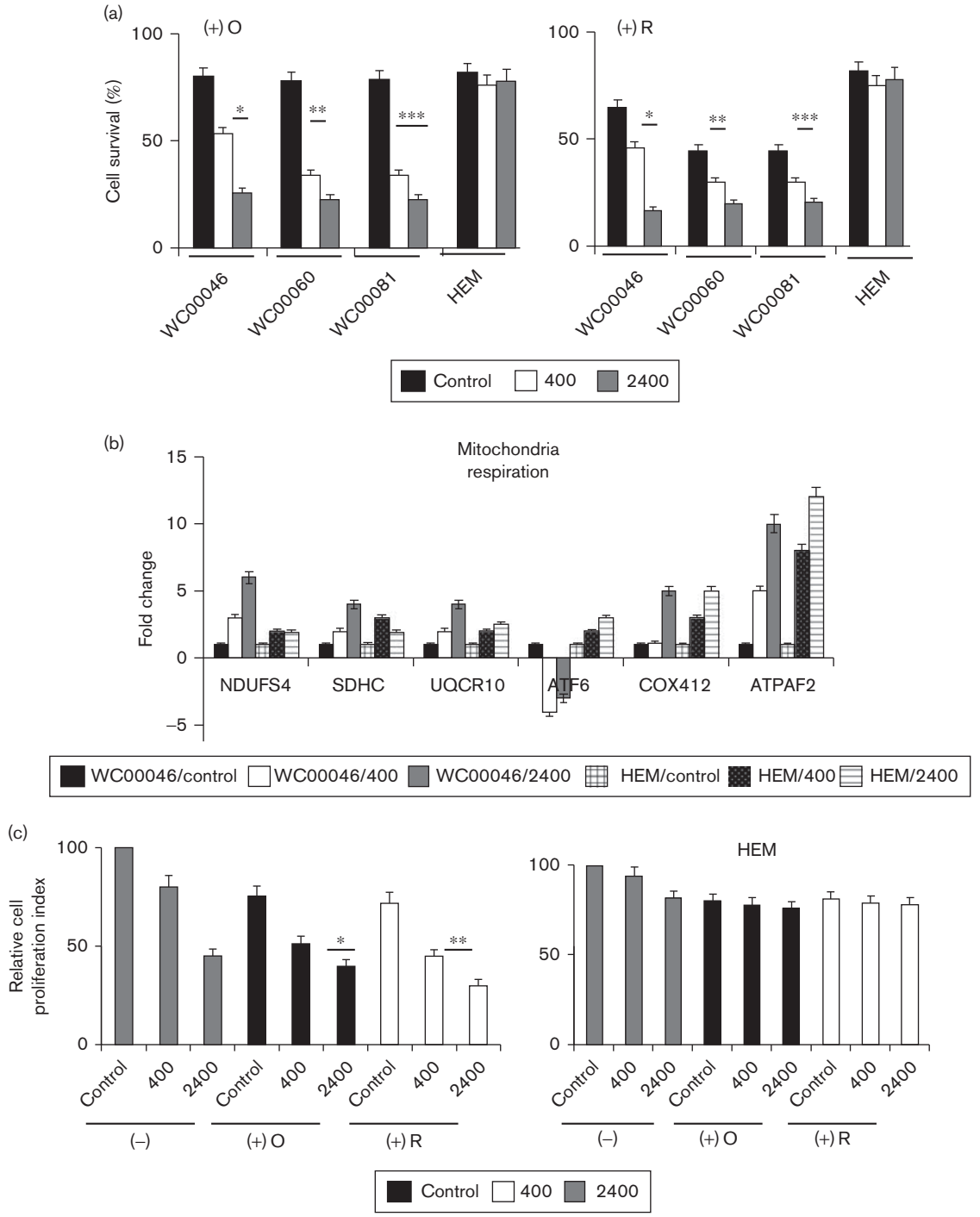

(a) Cells were pretreated with oligomycin [(+)O, 50 nmol/l] or rotenone [(+R), 50 nmol/l] for 1 h and subsequently irradiated with 0.5 Gy at either 400 MU/min (solid grey bars) or 2400 MU/min (solid white bars) compared with nonirradiated controls (solid black bars). At 7 days after irradiation, the number of surviving cells was counted and the percent survival was plotted after normalizing against corresponding control cells (means no radiation and no inhibitors = 100% survival, data not included in graph). The statistical differences between 400 and 2400 MU/min were $P < 0.008$ for WC00046 (*), $P < 0.001$ for WC00060 (**), and $P < 0.005$ for WC00081 (***) for (+)O and $P < 0.004$ for WC00046 (*), $P < 0.008$ for WC00081 (**), and $P < 0.005$ for WC00081 (***) for (+)R. (b) Gene expression was analyzed for mitochondrial respiration in irradiated cells by qRT-PCR. Gene expression data from WC00046/control, WC000/400, WC000/2400, HEM/control, HEM/400, and HEM/2400 are represented by solid black, solid white, solid grey, large grid, black-dotted, and light horizontal bars, respectively. (c) Proliferation potential was quantified using the MTT assay for WC00046 cells and HEM from (a) in the absence (control, solid grey bars) or presence of oligomycin [solid black bars, (+)O] or rotenone [solid white bars, (+)R] after irradiation with 0.5 Gy at 400 or 2400 MU/min. Statistical differences between the two dose rates were $P < 0.007$ for (+)O (*) and $P < 0.013$ for (+)R (**). All experiments were performed four times; standard error bars are shown. HEM, human epidermal melanocytes; qRT-PCR, quantitative real-time reverse transcriptase PCR.

quantified, irradiated WC00046 cells that were pretreated with inhibitors showed significant differences [11% for (+)O and 15% for (+)R] between the two dose rates; however, HEM cells did not show differences (Fig. 4c). Neither inhibitor significantly affected HEM survival, indicating that blocking mitochondrial respiration selectively enhances apoptosis of melanoma cells.

Colony survival of melanoma cells following irradiation at 2400 MU/min is significantly less than that after irradiation at 400 MU/min; however, HEM survival is maintained at 80%. To investigate the differences between cell-count data and end-point colony formation, irradiated cells were serially diluted and allowed to form colonies (Fig. 5a). The colony assay has been widely used in radiation biology to assess cytotoxicity and the effects of ionizing radiation on cells, as well as to study radiosensitizers [39,40]. Decreases in survival (%) of melanoma cells were observed from cell (Fig. 1c) and colony counts (Fig. 5b), suggesting that the apoptotic effect of ionizing radiation continued past 7 days after irradiation. In contrast to cancer cells, the colony and cell counts of HEM did not show significant differences, indicating that the normal cells recovered and proliferated immediately after radiation treatment. This was consistent with the reduction in or the absence of DNA damage after irradiation (Fig. 2). The colony formation assay indicated that cell killing efficiency following irradiation was three-fold greater for WC00046 cells, seven-fold greater for WC00060 cells, and two-fold greater for WC00081 cells at 2400 MU/min compared with 400 MU/min (Fig. 5b). HEM colonies maintained greater than 80% survival at both dose rates (Fig. 5b). Pretreatment with oligomycin and rotenone before radiation treatment further reduced survival of melanoma cells (average 21% and average 17%, respectively; Fig. 5c).

Protein expression analyses were carried out using anti-*Bcl-2*, anti-*caspase-3* (cleaved), and anti-*PARP 1* (cleaved) on untreated and irradiated melanoma cells for antiapoptotic and apoptotic signals, respectively. Expression of *Bcl-2* was downregulated in the irradiated melanoma cell lines (24 Gy/min), whereas untreated cells maintained their base level expressions (Fig. 6b). However, no significant changes were observed in the expression levels of caspase-3 between control and irradiated (24 Gy/min) cells (Fig. 6b). *PARP 1* protein levels in irradiated melanoma cells were minimally downregulated when compared with non-radiated controls. Flow cytometric analyses of *cyclin D1* and *cyclin D2* in melanoma cell lines 24 h after irradiation showed a minimal decrease in the expression of the cyclins (Fig. 6c).

Discussion

Melanoma is an aggressive skin cancer that kills more than 9000 people in the USA annually, and it was estimated that more than 76 000 new cases would be diagnosed in 2014 [41]. Melanoma is frequently radioresistant, and radiation protocols are effective only as palliative therapy. However, recent studies using external beam radiation therapy both *in vitro* and *in vivo* have demonstrated radioresponsiveness and a heterogeneous range of radiation sensitivities of melanoma [42–45]. Radiation therapy is infrequently used for treating primary tumors, but recent randomized data generated from high-risk patients suggest the importance of adjuvant radiotherapy [46]. Development of the FFF mode has improved radiotherapy for various cancers, including metastasized melanoma, with respect to both local control and palliation in patients [47,48]. To achieve better disease control and prevent progression of melanoma, we investigated the use of the FFF mode of irradiation to accelerate cell death in metastatic and malignant melanoma cell lines in an in-vitro setting. Our data demonstrated that the combination of an unconventional high dose rate (2400 MU/min) with a low total dose (0.5 Gy) in the FFF mode produced greater induction of apoptosis in melanoma cells than that obtained with a conventional clinical dose rate (400 MU/min). This protocol produced an average of five-fold more cell death in the in-vitro setting, implying that a similar clinical protocol could be derived that would minimize long-term toxicities resulting from high radiation doses [49]. Minimizing toxicities is a major goal of anticancer therapy. With our protocol using a low overall dose but a high dose rate, survival of HEM and HDF were preserved above 80% (Figs 1 and 5). Recently, intensity-modulated radiotherapy for mucosal melanoma yielded a 3-year survival rate and mild toxicity for 75% of patients [50], implying that our unconventional radiation protocol has translational potential to the clinical setting.

High-dose radiation causes extensive damage to normal tissue surrounding the tumor, thereby inducing lesions and prolonging toxic side effects [51]. Unfortunately, the adverse untargeted effects of radiotherapy include alterations to the microenvironment of the target tissue, induction of metastasis, and worsening of clinical outcome [52]. There is an unmet clinical need for delivering low-dose radiation and maintaining a low total radiotherapeutic dose. In our experimental setting, delivery of 0.5 Gy in combination with a high dose rate of 2400 MU/min had minimal cellular radiotoxicity in HEM and HDF while accelerating the killing of melanoma cells. Significant upregulation of apoptotic genes in melanoma cells confirmed these findings. Radiation-mediated DNA damage and cell death of melanoma cells were evident immediately, but the data also indicate that the toxic effect continued, as cell survival determined from colony counts was significantly less than that predicted from the cell count at 7 days after irradiation. In contrast, HEM and HDF showed nonsignificant radiotoxicity. Our data indicate that this radioprotection may be a consequence of overexpression of DNA repair genes

Fig. 5

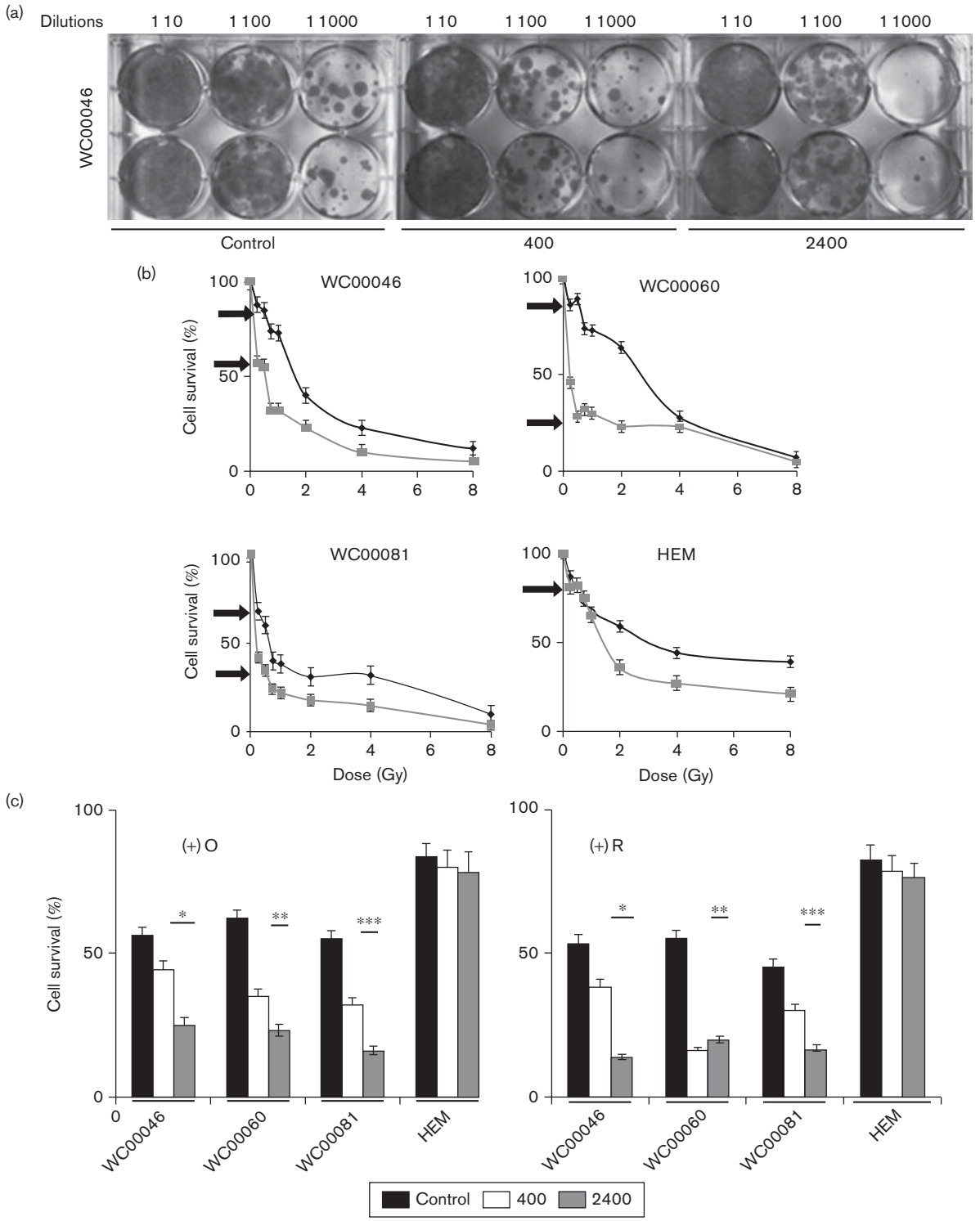

(a) Colony assays were performed for each radiation treatment. Cells were serially diluted in six-well plates in duplicate. Stained colonies of WC00046 cells under the dose rates 400 and 2400 MU/min with 0.5 Gy total dose are shown next to nonradiated controls. WC00060 and WC00081 colonies showed similar staining (data not shown). (b) Percent cell survival of irradiated cells that received 0.25, 0.5, 0.75, 1, 2, 4, or 8 Gy at 400 MU/min (solid black line with diamond) or 2400 MU/min (solid gray line with square) was plotted by counting colonies. Arrows indicate a 0.5 Gy total dose for both dose rates. (c) Percent cell survival of irradiated cells from (b) that received a 0.5 Gy total dose plotted after normalizing against corresponding untreated controls (100% cell survival means no radiation, no inhibitors; data not shown). Percent cell survivals are shown in the absence (solid black bars) and presence (solid grey bars for 400 MU/min and solid white bars for 2400 MU/min) of the mitochondrial respiration inhibitors oligomycin [(+)O] and rotenone [+(R)]. All experiments were performed four times separately; standard error bars are shown.

Fig. 6

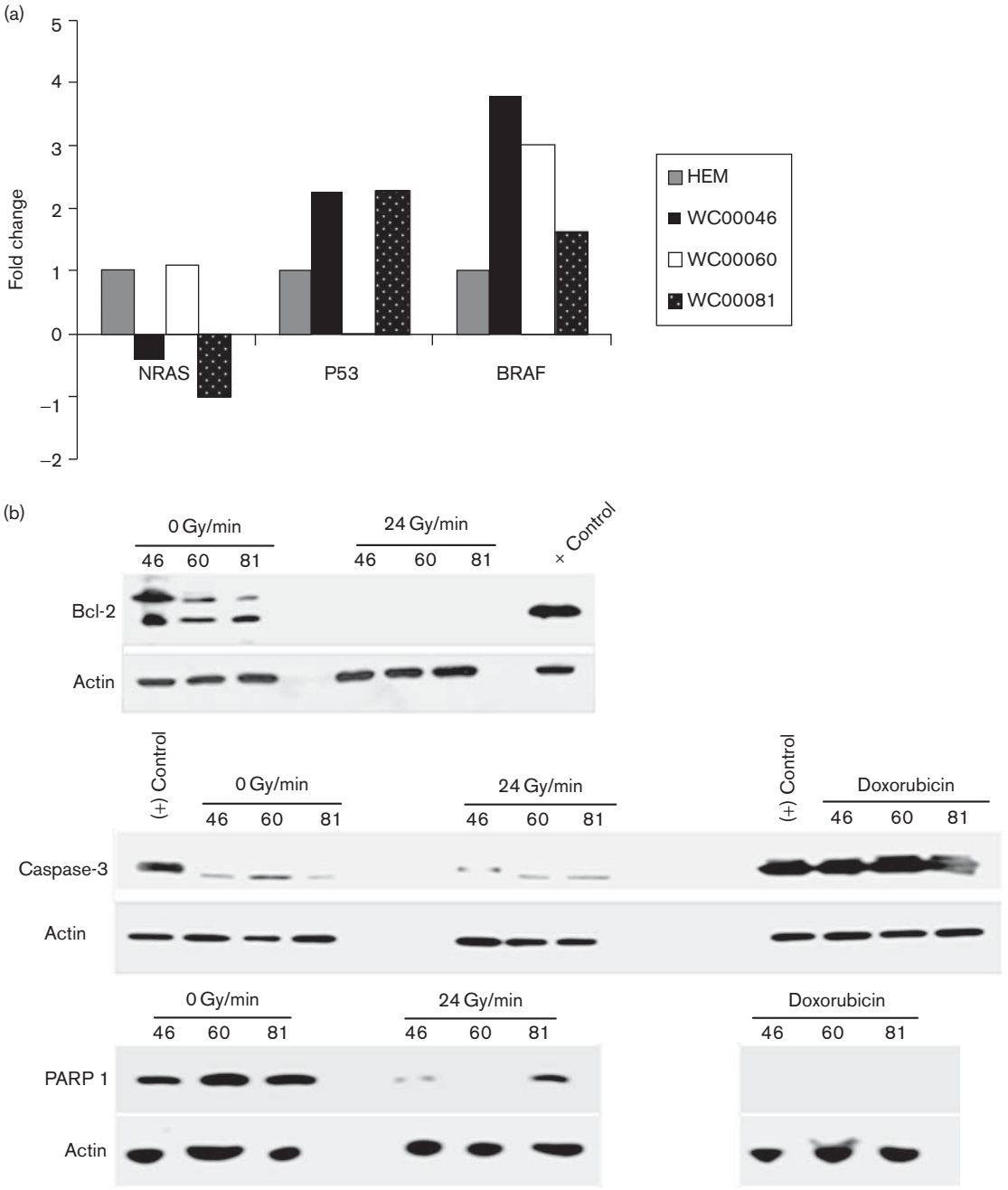

(a) Mutational status of NRAS, p53, and BRAF genes in melanoma cell lines was tested using qRT-PCR analysis. Cell lines WC00046, WC00060, and WC00081 are represented by solid black, solid white, dotted black bars. (b)Western blot analysis of Bcl-2 (1 : 1000), PARP 1 (1 : 2000), and caspase-3 (1 : 2000) was carried out on 12% SDS-PAGE gels and the whole-cell extracts were transferred onto a PVDF membrane. The membranes were washed and incubated with a 1 : 5000 dilution of horseradish peroxidase-conjugated donkey anti-mouse IgG. The blots were washed and developed using the ECL system. (c) Analysis of cyclin D1 and cyclin D2 expressions in melanoma cell lines was carried out with PE-labeled antibodies using flow cytometry. A total of 1×10^6 cells from control and irradiated groups were harvested from T-25 flasks 24 h after radiation by centrifugation at 1200 rpm for 7 min, and cell pellets were washed with ice cold PBS. The Per Fix-nc kit was used for fixing, permeabilizing, and preparing the cells for the assay. HEM, human epidermal melanocytes; PVDF, polyvinylidene difluoride; qRT-PCR, quantitative real-time reverse transcriptase PCR.

and minimal DNA damage (Fig. 2). In addition, the cell proliferation potential of HEM and HDF was not altered by radiation; instead, the cells showed significant upregulation of cyclins to promote cell division for recovery after 7 days. Moreover, the levels of the proteins *cyclin D1* and *cyclin D2* in melanoma cells 1 day after

Fig. 6 (*Continued*)

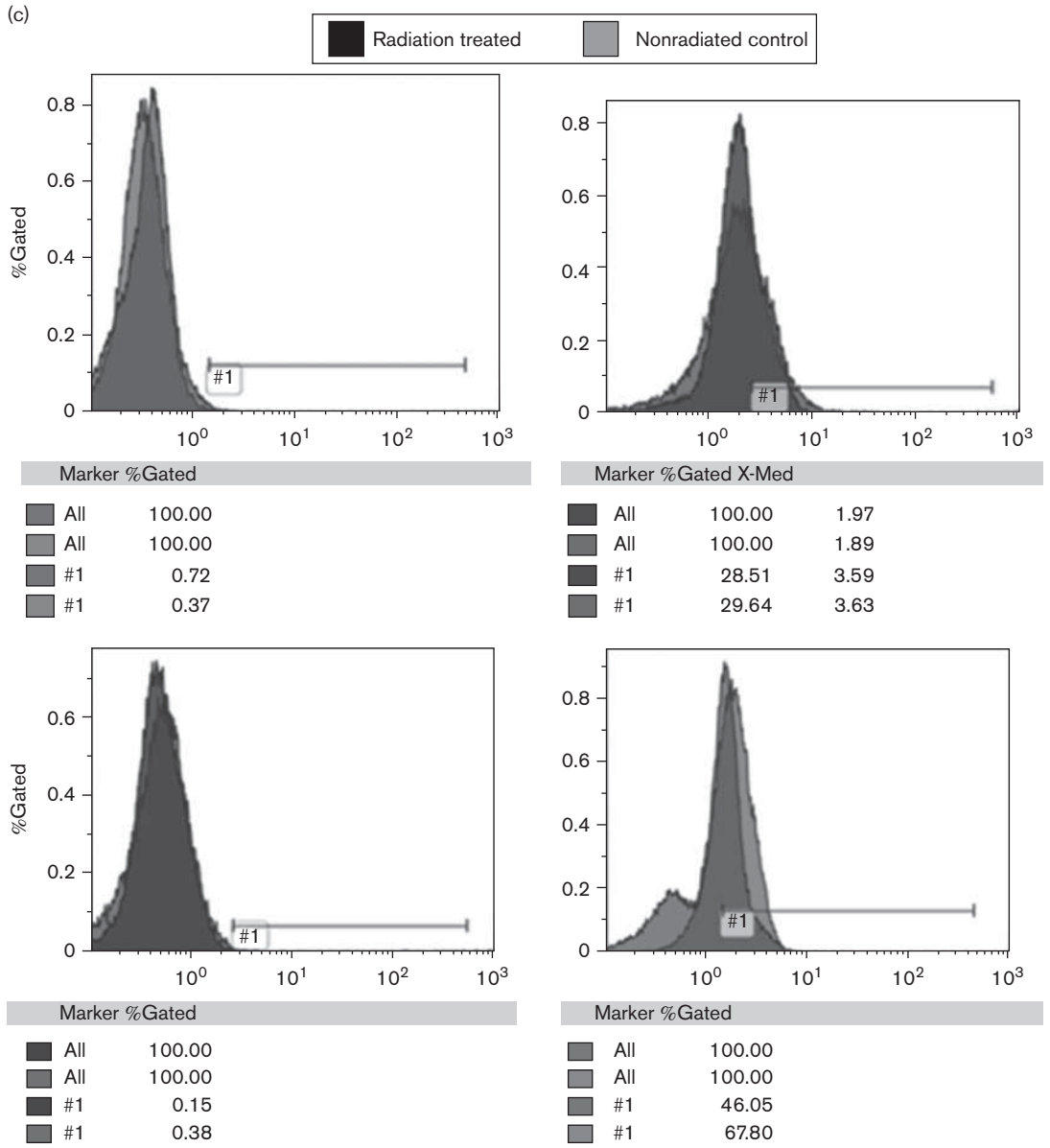

irradiation (24 Gy/min) were minimally decreased compared with that in nonradiated controls, indicating that the process of apoptosis had begun soon after irradiation, consistent with downregulation of Bcl-2 in the irradiated (24 Gy/min) melanoma samples. These *in-vitro* data provide evidence that use of the FFF mode, a dose rate of 2400 MU/min, and a low total dose of 0.5 Gy can potentially fulfill clinical needs and enhance clinical outcomes.

Mitochondrial function is directly related to cancer progression [53,54]. Our data showed that radiation caused melanoma cells to upregulate mitochondrial respiration, and this active energy production may be associated with a radioprotective mechanism (Fig. 3). Furthermore, proteinalysis of caspase-3 (cleaved) and PARP 1 (cleaved) showed no significant difference in melanoma cells in both nonradiated and irradiated (24 Gy/min) samples (Fig. 6b). Respiratory activity was directly correlated with dose rate in cancer cells up to 7 days after irradiation; however, this was not observed in HEM and HDF, suggesting apoptotic pressure on cancer cells but not on primary normal cells. Radiation-mediated mitochondrial respiratory activities in melanoma cells can be efficiently blocked by oligomycin or rotenone in dose windows that are minimally toxic to primary skin cells (Fig. 3), demonstrating potential efficacy for managing melanoma in combination with selected radiotherapy protocols.

Previous studies have shown that sensitization of mitochondrial pathways in melanoma induces responses to chemotherapeutics [55]. Furthermore, the metabolic pathways of normal cells depend on oxidative phosphorylation, but cancer cells rely on aerobic glycolysis, which depends on mitochondrial respiration [56]. The results of this in-vitro study give a new perspective to melanoma therapy – that is, the combinatorial effect of high dose rate and low total dose has higher apoptotic potential in melanoma cells but minimal deleterious effects on surrounding HEM. Moreover, the addition of mitochondrial inhibitors further enhances apoptosis in melanoma while retaining high survival percentages of HEM, indicating a beneficial role of mitochondrial inhibitors in adjuvant therapy for metastatic and malignant melanomas. Innovative technology developments help deliver the required doses to the tumor and minimize damage to the surrounding tissue [57]. In this study, mitochondrial inhibitors were shown to have a significant influence on melanoma radiation therapy, reducing survival of metastatic melanoma cells to 25% in colony assays and 44% in cell-count assays, and maintaining 80% survival of HEM.

Our results demonstrate that radiation at a dose rate of 2400 MU/min enhances apoptosis in melanoma cells through a Fas-mediated apoptotic pathway (Fig. 1d). The activation of Fas and a cascade of several apoptotic genes triggers apoptosis in melanoma cells. Fas-mediated apoptotic signaling in melanoma cells has been documented previously [58]. The underlying mechanism for the activation Fas signaling by a high dose rate of radiation is not known, and further study is required. Downregulation of antiapoptotic genes and upregulation of apoptotic and stress genes in ER and cell-death pathways support the high cell-kill efficiency of the 2400 MU/min dose rate compared with the conventional clinical dose rate of 400 MU/min. The absence of differential expression of these genes in primary skin cells suggests that the total dose of 0.5 Gy under both dose rates was relatively harmless.

In summary, this study demonstrates a potential anti-melanoma therapy by using a combination of high dose rate and low total dose (2400 MU/min/0.5 Gy) to enhance the radiosensitivity and apoptotic rates in melanoma cells while preserving the survival of primary skin cells. The radiosensitivity can be further increased by inhibiting the activities of mitochondrial respiration chains. Melanoma cells upregulate mitochondrial respiration to partly overcome the damage caused by radiation treatment. The combinatorial use of a dose rate 2400 MU/min, a low dose of 0.5 Gy, and blockers of mitochondrial respiration activity can potentially introduce innovative anti-melanoma therapeutic options in the clinical setting.

Acknowledgements

The authors thank the radiotherapists and radiation physicists of the John Theurer Cancer Center, Hackensack University Medical Center (Hackensack, New Jersey, USA) for their continuous support and help in carrying out irradiation using TrueBeam, which was required for this study. They also thank Rana, Michael Jones, and Irfan Qureshi for helping with irradiation and preparation of TrueBeam. This study was funded by the John Theurer Cancer Center (Hackensack University Medical Center, New Jersey, USA).

Conflicts of interest

There are no conflicts of interest.

References

1 Markovic SN, Erickson LA, Rao RD, Weenig RH, Pockaj BA, Bardia A, *et al.* Malignant melanoma in the 21st century, part 2: staging, prognosis, and treatment. *Mayo Clin Proc* 2007; **82**:490–513.
2 Bandarchi B, Jabbari CA, Vedadi A, Navab R. Molecular biology of normal melanocytes and melanoma cells. *J Clin Pathol* 2013; **66**:644–648.
3 Wadasadawala T, Trivedi S, Gupta T, Epari S, Jalali R. The diagnostic dilemma of primary central nervous system melanoma. *J Clin Neurosci* 2010; **17**:1014–1017.
4 Dye DE, Medic S, Ziman M, Coombe DR. Melanoma biomolecules: independently identified but functionally intertwined. *Front Oncol* 2013; **3**:252.
5 Lejeune FJ, Rimoldi D, Speiser D. New approaches in metastatic melanoma: biological and molecular targeted therapies. *Expert Rev Anticancer Ther* 2007; **7**:701–713.
6 Goulart CR, Mattei TA, Ramina R. Cerebral melanoma metastases: a critical review on diagnostic methods and therapeutic options. *ISRN Surg* 2011; **2011**:276908.
7 Forschner A, Heinrich V, Pflugfelder A, Meier F, Garbe C. The role of radiotherapy in the overall treatment of melanoma. *Clin Dermatol* 2013; **31**:282–289.
8 Stevens G, McKay MJ. Dispelling the myths surrounding radiotherapy for treatment of cutaneous melanoma. *Lancet Oncol* 2006; **7**:575–583.
9 Walls AC, Han J, Li T, Qureshi AA. Host risk factors, ultraviolet index of residence, and incident malignant melanoma in situ among US women and men. *Am J Epidemiol* 2013; **177**:997–1005.
10 Davies H, Bignell GR, Cox C, Stephens P, Edkins S, Clegg S, *et al.* Mutations of the BRAF gene in human cancer. *Nature* 2002; **417**:949–954.
11 Kolch W. Meaningful relationships: the regulation of the Ras/Raf/MEK/ERK pathway by protein interactions. *Biochem J* 2000; **351 Pt 2** (Pt 2):289–305.
12 Calipel A, Lefevre G, Pouponnot C, Mouriaux F, Eychène A, Mascarelli F. Mutation of B-Raf in human choroidal melanoma cells mediates cell proliferation and transformation through the MEK/ERK pathway. *J Biol Chem* 2003; **278**:42409–42418.
13 Khan MK, Khan N, Almasan A, Macklis R. Future of radiation therapy for malignant melanoma in an era of newer, more effective biological agents. *Onco Targets Ther* 2011; **4**:137–148.
14 Colombino M, Capone M, Lissia A, Cossu A, Rubino C, De Giorgi V, *et al.* BRAF/NRAS mutation frequencies among primary tumors and metastases in patients with melanoma. *J Clin Oncol* 2012; **30**:2522–2529.
15 McCubrey JA, Steelman LS, Abrams SL, Lee JT, Chang F, Bertrand FE, *et al.* Roles of the RAF/MEK/ERK and PI3K/PTEN/AKT pathways in malignant transformation and drug resistance. *Adv Enzyme Regul* 2006; **46**:249–279.
16 Eckerle Mize D, Bishop M, Resse E, Sluzevich J. Familial atypical multiple mole melanoma syndrome. In: Riegert-Johnson DL, Boardman LA, Hefferon T, Roberts M, editors. *Cancer Syndromes*. Bethesda, MD: National Centre for Biotechnology Information (US); 2009.
17 Peralta-Leal A, Rodríguez MI, Oliver FJ. Poly(ADP-ribose)polymerase-1 (PARP-1) in carcinogenesis: potential role of PARP inhibitors in cancer treatment. *Clin Transl Oncol* 2008; **10**:318–323.
18 Barranco SC, Romsdahl MM, Humphrey RM. The radiation response of human malignant melanoma cells grown in vitro. *Cancer Res* 1971; **31**:830–833.
19 Sharma SD. Unflattened photon beams from the standard flattening filter free accelerators for radiotherapy: advantages, limitations and challenges. *J Med Phys* 2011; **36**:123–125.
20 Rana S. Intensity modulated radiation therapy versus volumetric intensity modulated arc therapy. *J Med Radiat Sci* 2013; **60**:81–83.
21 Balcer-Kubiczek EK. Apoptosis in radiation therapy: a double-edged sword. *Exp Oncol* 2012; **34**:277–285.

22 Xu X, Duan S, Yi F, Ocampo A, Liu GH, Izpisua Belmonte JC. Mitochondrial regulation in pluripotent stem cells. *Cell Metab* 2013; **18**:325–332.
23 Dhillon VS, Fenech M. Mutations that affect mitochondrial functions and their association with neurodegenerative diseases. *Mutat Res Rev Mutat Res* 2014; **759**:1–13.
24 Gogvadze V, Orrenius S, Zhivotovsky B. Mitochondria in cancer cells: what is so special about them? *Trends Cell Biol* 2008; **18**:165–173.
25 Kam WW, Banati RB. Effects of ionizing radiation on mitochondria. *Free Radic Biol Med* 2013; **65**:607–619.
26 Suh KS, Mutoh M, Mutoh T, Li L, Ryscavage A, Crutchley JM*, et al.* CLIC4 mediates and is required for Ca^{2+}-induced keratinocyte differentiation. *J Cell Sci* 2007; **120** (Pt 15):2631–2640.
27 Pajoum Shariati SR, Shokrgozar MA, Vossoughi M, Eslamifar A. In vitro co-culture of human skin keratinocytes and fibroblasts on a biocompatible and biodegradable scaffold. *Iran Biomed J* 2009; **13**:169–177.
28 Godwin LS, Castle JT, Kohli JS, Goff PS, Cairney CJ, Keith WN*, et al.* Isolation, culture, and transfection of melanocytes. *Curr Protoc Cell Biol* 2014; **63**:1.8.1–1.8.20.
29 Franken NA, Rodermond HM, Stap J, Haveman J, van Bree C. Clonogenic assay of cells in vitro. *Nat Protoc* 2006; **1**:2315–2319.
30 Munshi A, Hobbs M, Meyn RE. Clonogenic cell survival assay. *Methods Mol Med* 2005; **110**:21–28.
31 Zhu S, Oremo JA, Li S, Zhen M, Tang Y, Du Y. Synergistic antitumor activities of docetaxel and octreotide associated with apoptotic-upregulation in castration-resistant prostate cancer. *PLoS One* 2014; **9**:e91817.
32 Lu R, Gao H, Wang H, Cao L, Bai J, Zhang Y. Overexpression of the Notch3 receptor and its ligand Jagged1 in human clinically non-functioning pituitary adenomas. *Oncol Lett* 2013; **5**:845–851.
33 Zhao J, Xiang Y, Xiao C, Guo P, Wang D, Liu Y, Shen Y. AKR1C3 overexpression mediates methotrexate resistance in choriocarcinoma cells. *Int J Med Sci* 2014; **11**:1089–1097.
34 Mahmood T, Yang PC. Western blot: technique, theory, and trouble shooting. *N Am J Med Sci* 2012; **4**:429–434.
35 Kotecha N, Krutzik PO, Irish JM. Web-based analysis and publication of flow cytometry experiments. *Curr Protoc Cytom* 2010; **Chapter 10**:Unit10.17.
36 Menon V, Thomas R, Ghale AR, Reinhard C, Pruszak J. Flow cytometry protocols for surface and intracellular antigen analyses of neural cell types. *J Vis Exp* 2014. Available at: *http://www.jove.com/video/52241/flow-cytometry-protocols-for-surface-intracellular-antigen-analyses* [Accessed 6 July 2015].
37 Murley JS, Kataoka Y, Baker KL, Diamond AM, Morgan WF, Grdina DJ. Manganese superoxide dismutase (SOD2)-mediated delayed radioprotection induced by the free thiol form of amifostine and tumor necrosis factor alpha. *Radiat Res* 2007; **167**:465–474.
38 Leach JK, Black SM, Schmidt-Ullrich RK, Mikkelsen RB. Activation of constitutive nitric-oxide synthase activity is an early signaling event induced by ionizing radiation. *J Biol Chem* 2002; **277**:15400–15406.
39 Wallace DC. Mitochondria and cancer. *Nat Rev Cancer* 2012; **12**:685–698.
40 Baraldi MM, Alemi AA, Sethna JP, Caracciolo S, La Porta CA M, Zapperi Stefano. Growth and form of melanoma cell colonies. *J Stat Mech* 2013; **2013**:P02032.
41 Siegel R, Ma J, Zou Z, Jemal A. Cancer statistics, 2014. *CA Cancer J Clin* 2014; **64**:9–29.
42 Rofstad EK. Radiation sensitivity in vitro of primary tumors and metastatic lesions of malignant melanoma. *Cancer Res* 1992; **52**:4453–4457.
43 Rofstad EK. Radiation biology of malignant melanoma. *Acta Radiol Oncol* 1986; **25**:1–10.
44 Strojan P. Role of radiotherapy in melanoma management. *Radiol Oncol* 2010; **44**:1–12.
45 Sambade MJ, Peters EC, Thomas NE, Kaufmann WK, Kimple RJ, Shields JM. Melanoma cells show a heterogeneous range of sensitivity to ionizing radiation and are radiosensitized by inhibition of B-RAF with PLX-4032. *Radiother Oncol* 2011; **98**:394–399.
46 Rao NG, Yu HH, Trotti A 3rd, Sondak VK. The role of radiation therapy in the management of cutaneous melanoma. *Surg Oncol Clin N Am* 2011; **20**:115–131.
47 Olivier KR, Schild SE, Morris CG, Brown PD, Markovic SN. A higher radiotherapy dose is associated with more durable palliation and longer survival in patients with metastatic melanoma. *Cancer* 2007; **110**:1791–1795.
48 Berk LB. Radiation therapy as primary and adjuvant treatment for local and regional melanoma. *Cancer Control* 2008; **15**:233–238.
49 Lengua RE, Gonzalez MF, Barahona K, Ixquiac ME, Lucero JF, Montenegro E*, et al.* Toxicity outcome in patients treated with modulated arc radiotherapy for localized prostate cancer. *Rep Pract Oncol Radiother* 2014; **19**:234–238.
50 Combs SE, Konkel S, Thilmann C, Debus J, Schulz-Ertner D. Local high-dose radiotherapy and sparing of normal tissue using intensity-modulated radiotherapy (IMRT) for mucosal melanoma of the nasal cavity and paranasal sinuses. *Strahlenther Onkol* 2007; **183**:63–68.
51 Chapel A, Francois S, Douay L, Benderitter M, Voswinkel J. Fifteen years of preclinical and clinical experiences about biotherapy treatment of lesions induced by accidental irradiation and radiotherapy. *World J Stem Cells* 2013; **5**:68–72.
52 Shin JW, Son JY, Raghavendran HR, Chung WK, Kim HG, Park HJ*, et al.* High-dose ionizing radiation-induced hematotoxicity and metastasis in mice model. *Clin Exp Metastasis* 2011; **28**:803–810.
53 Maes H, Agostinis P. Autophagy and mitophagy interplay in melanoma progression. *Mitochondrion* 2014; **19 Pt A**:58–68.
54 Gaude E, Frezza C. Defects in mitochondrial metabolism and cancer. *Cancer Metab* 2014; **2**:10.
55 Gembarska A, Luciani F, Fedele C, Russell EA, Dewaele M, Villar S*, et al.* MDM4 is a key therapeutic target in cutaneous melanoma. *Nat Med* 2012; **18**:1239–1247.
56 Perez CA, Mutic S. Advances and future of radiation oncology. *Rep Pract Oncol Radiother* 2013; **18**:329–332.
57 Ramsay EE, Hogg PJ, Dilda PJ. Mitochondrial metabolism inhibitors for cancer therapy. *Pharm Res* 2011; **28**:2731–2744.
58 Shukuwa T, Katayama I, Koji T. Fas-mediated apoptosis of melanoma cells and infiltrating lymphocytes in human malignant melanomas. *Mod Pathol* 2002; **15**:387–396.